X-ray observations of FO Aqr during the 2016 low state

M. R. Kennedy, P. M. Garnavich, C. Littlefield, P. Callanan, K. Mukai, E. Aadland, M. Kotze, E. Kotze

June 8th 2017

Forms of accretion

Magnetic fields are capable of truncating accretion discs at a radius of

$$r_M = \left(\frac{8\pi^2 R_1^{12}}{\mu^2 G M_1} \frac{B_s^4}{\dot{m}^2} \right)^{\frac{1}{7}}$$

Hence, the magnetic field plays a very important role in accretion.

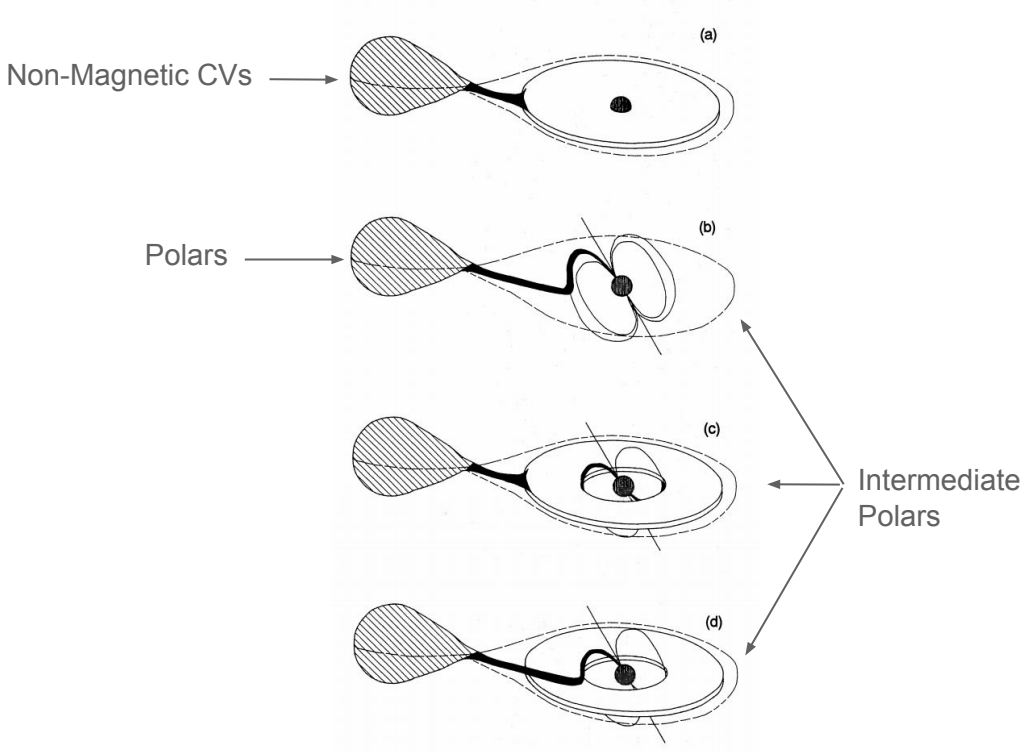

Norton, A. J. 1993, MNRAS, 265, 316

Pulses from intermediate polars (magnetic systems)

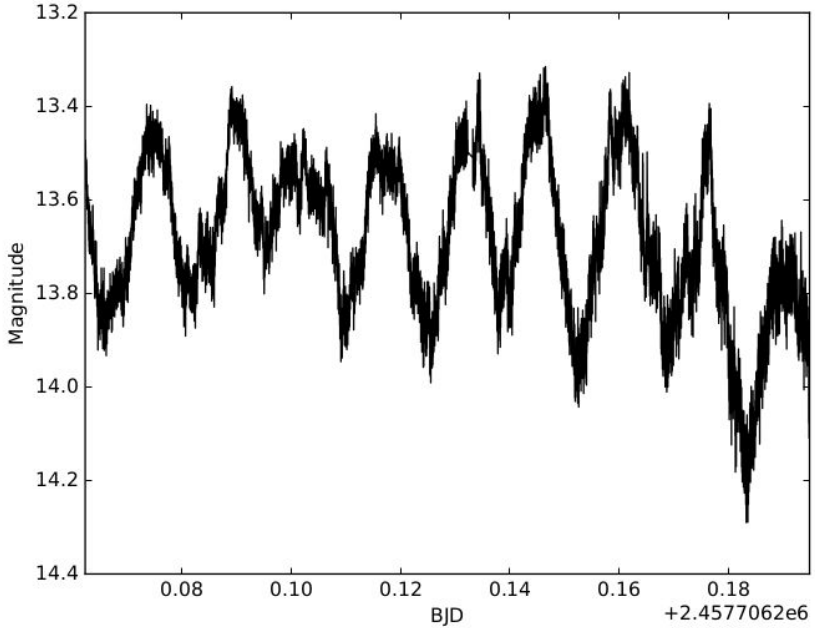

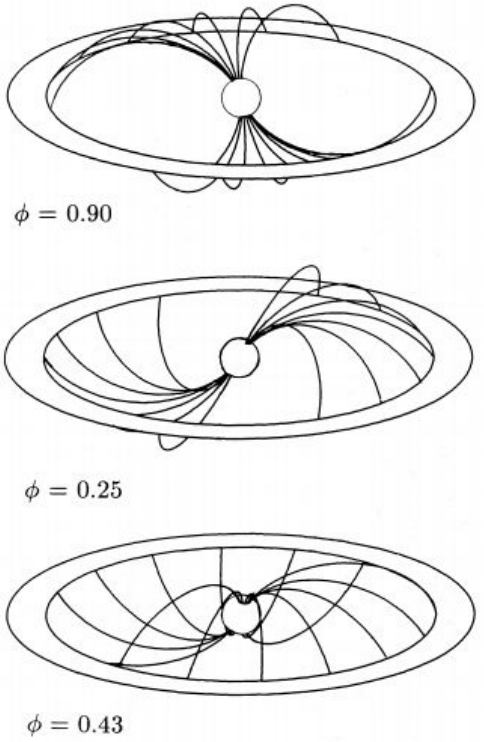

Hellier, Cropper & Mason, 1991, MNRAS, 248, 233

The fall and rise of the intermediate polar FO Aquarii

M. R. Kennedy et al., 2016, MNRAS, 459, 3622
C. Littlefield et al., 2016, ApJ, 833, 93
M. R. Kennedy et al., 2017, MNRAS, 469, 596

Background

FO Aquarii (FO Aqr) is an intermediate polar with a spin period of 20 mins and an orbital period of 4 hours

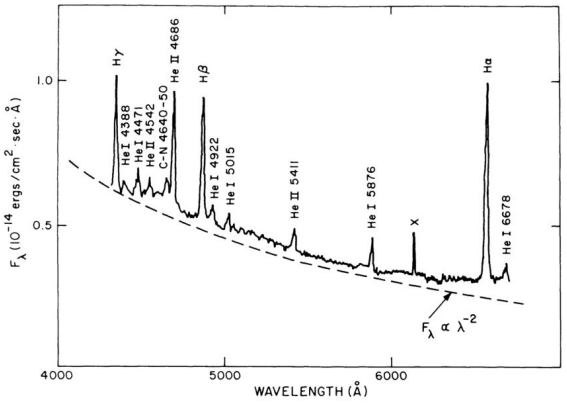

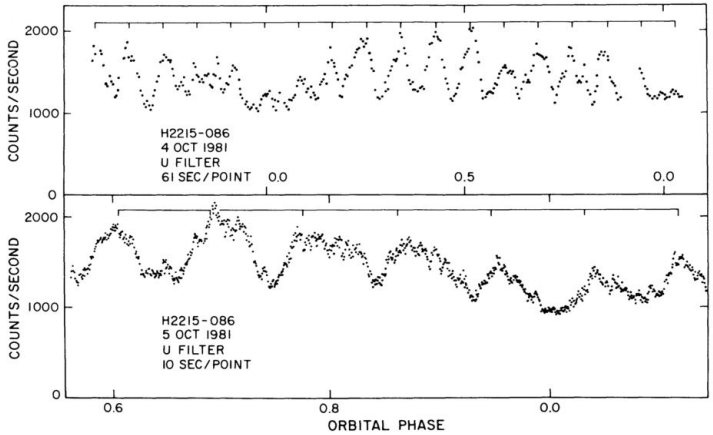

Patterson, J., & Steiner, J., 1983,
ApJ, 264, L61

History of the Spin Period

In 1982, spin period of 1254.4514(3) s and was increasing (Shafter & Macry 1987)

In 1987, spin period of 1254.4511(4) s and was steady (Steiman-Cameron, Imamura & Steiman-Cameron (1989))

In 1998, spin period of 1254.4446(2) s and was decreasing (Kruszewski & Semeniuk 1998; Patterson et al. 1998)

In 2003, spin period of 1254.4441(1) s (Williams 2003)

In 2004, spin period of 1254.284(16) s (Andronov, Ostrova & Burwitz 2005).

Kepler K2 observations of FO Aqr

Observed as part of campaign 3 of the K2 mission from Nov 14 2014 - Feb 3 2015 with a cadence of 1 min.

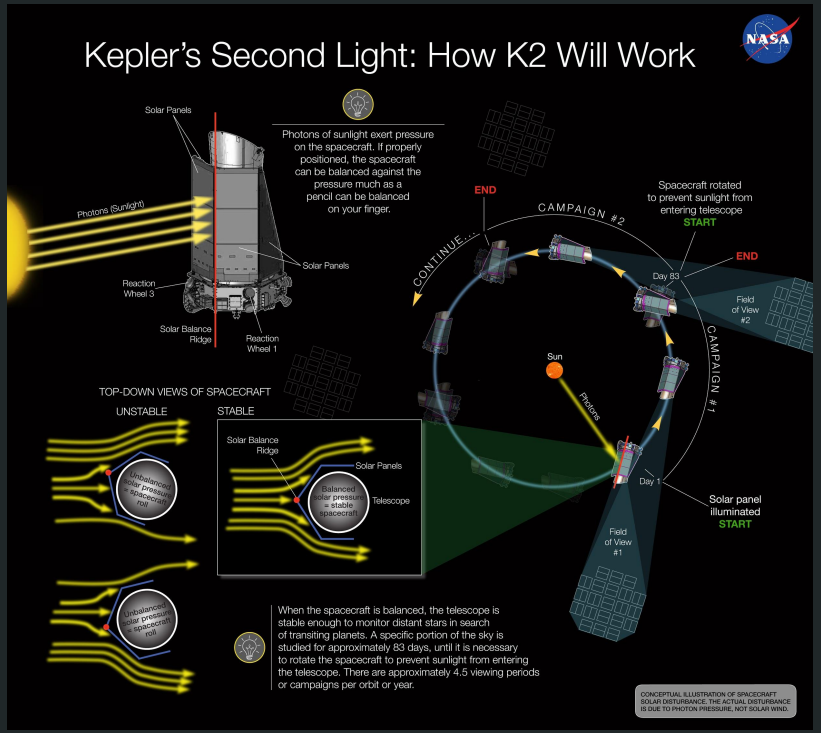

Extracted light curve of FO Aqr

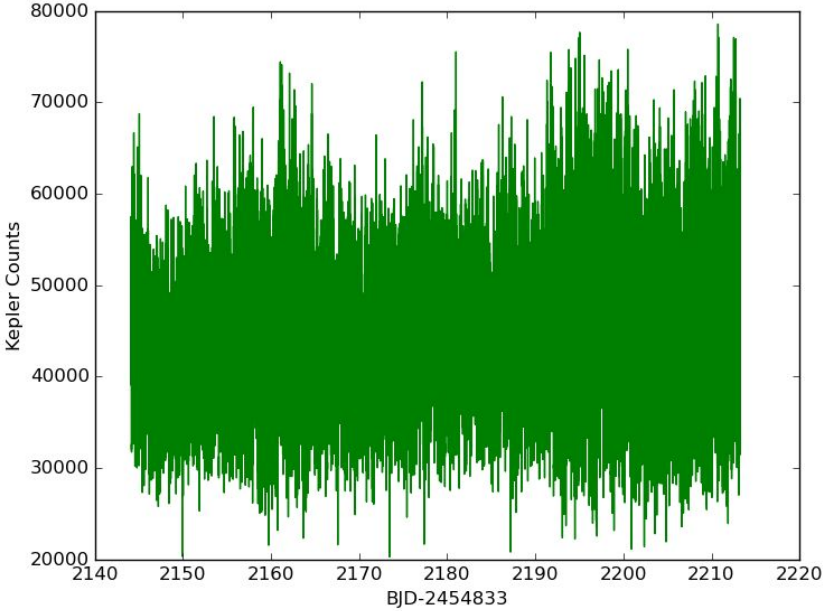

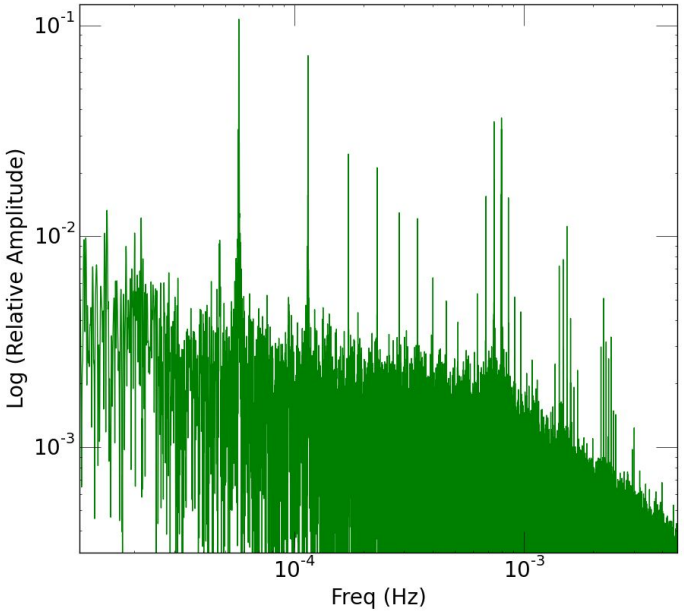

Power Spectrum of 69 day light curve

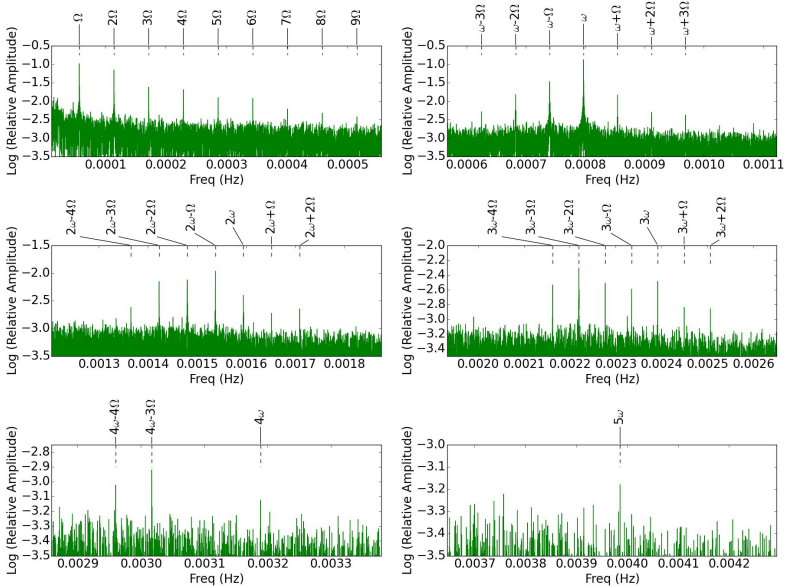

Strong power at orbital frequency and spin frequency, and many harmonics detected

	Frequency Hz ($\times 10^{-4}$)	Period (h)	Relative amplitude
Ω	0.572 65(4)	4.8508(4)	0.101(4)
2Ω	1.1456(8)	2.425(3)	0.071(3)
3Ω	1.7185(8)	1.6164(8)	0.0240(3)
4Ω	2.2912(8)	1.2123(4)	0.0208(3)
5Ω	2.8639(9)	0.9699(3)	0.0126(3)
6Ω	3.4369(8)	0.8082(2)	0.0118(2)
7Ω	4.007(1)	0.6928(2)	0.0061(2)
8Ω	4.5825(8)	0.6062(1)	0.0048(1)
9Ω	5.1547(9)	0.5389(1)	0.0038(1)
		(s)	
ω	7.972 319(2)	1254.3401(4)	0.1367(4)
$\omega-\Omega$	7.400 15(1)	1351.329(2)	0.0282(4)
$\omega+\Omega$	8.545 09(1)	1170.262(2)	0.0205(4)
$\omega-2\Omega$	6.826 52(1)	1464.876(2)	0.0222(4)
$\omega+2\Omega$	9.1179(8)	1096.74(6)	0.0050(3)
$\omega-3\Omega$	6.2541(8)	1599.0(2)	0.0052(3)
$\omega+3\Omega$	9.6907(8)	1031.94(6)	0.0042(2)
2ω	15.9443(8)	627.18(3)	0.0040(2)
$2\omega-\Omega$	15.3721(9)	650.53(4)	0.0107(3)
$2\omega+\Omega$	16.5177(9)	605.41(4)	0.001 85(3)
$2\omega-2\Omega$	14.7993(9)	675.71(4)	0.0075(3)
$2\omega+2\Omega$	17.090(1)	585.12(4)	0.0023(2)
$2\omega-3\Omega$	14.2267(8)	702.91(4)	0.0071(3)
$2\omega-4\Omega$	13.6539(8)	732.39(4)	0.0024(2)
3ω	23.9171(9)	418.11(2)	0.0032(2)
$3\omega-\Omega$	23.3443(9)	428.37(2)	0.0025(2)
$3\omega+\Omega$	24.490(1)	408.34(2)	0.0014(1)
$3\omega-2\Omega$	22.7714(8)	439.15(2)	0.0030(2)
$3\omega+2\Omega$	25.0628(8)	399.00(1)	0.0013(1)
$3\omega-3\Omega$	22.1991(8)	450.47(2)	0.0048(4)
$3\omega-4\Omega$	21.6258(8)	462.71(2)	0.0029(2)
4ω	31.8880(9)	313.58(1)	0.000 75(1)
$4\omega-3\Omega$	30.1714(9)	331.44(1)	0.001 20(3)
$4\omega-4\Omega$	29.5987(8)	337.85(1)	0.000 95(3)
5ω	39.862(1)	250.87 (1)	0.000 65(1)

A change in the spin period

Our published spin period of 1254.3401(4) s in 2016 was significantly longer than the last period of 1254.284(16) - suggested the WD was spinning down.

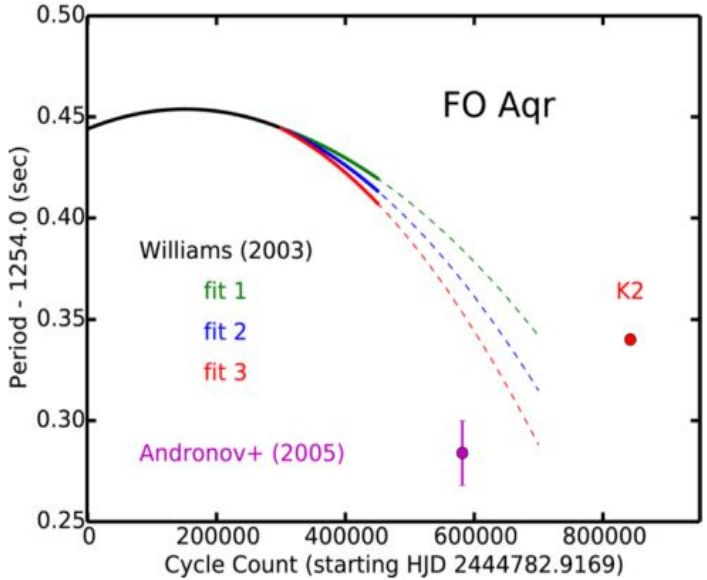

Update to the spin period

The phase-brightness correlation caused an overestimate in the spin period due to the limitations of how a power spectra is implemented.

Actual spin period of FO Aqr was found to be

1254.3342(8) s

by combining the Kepler data with other data taken between 2014 and 2016 (Bonnardeau 2016)

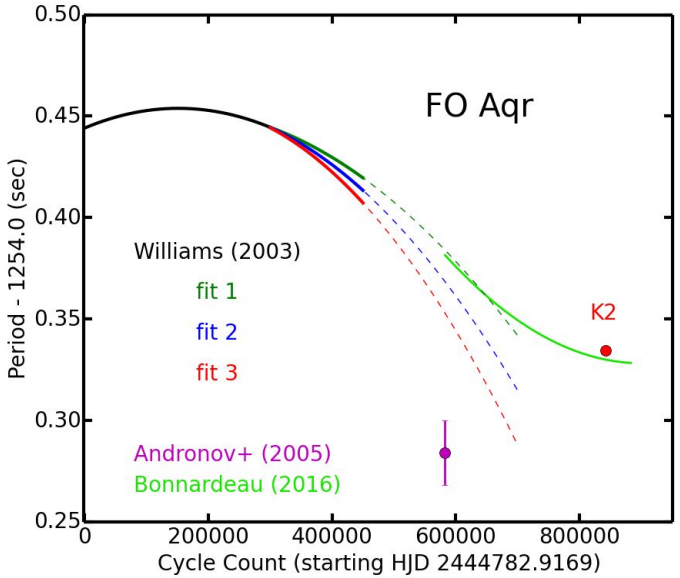

Changing Accretion Geometries

The increase in the amplitude of the beat period towards the end of the observations (along with the increase in flux) suggests the system temporarily transitioned from a simply disc-fed system to a disc-overflow geometry

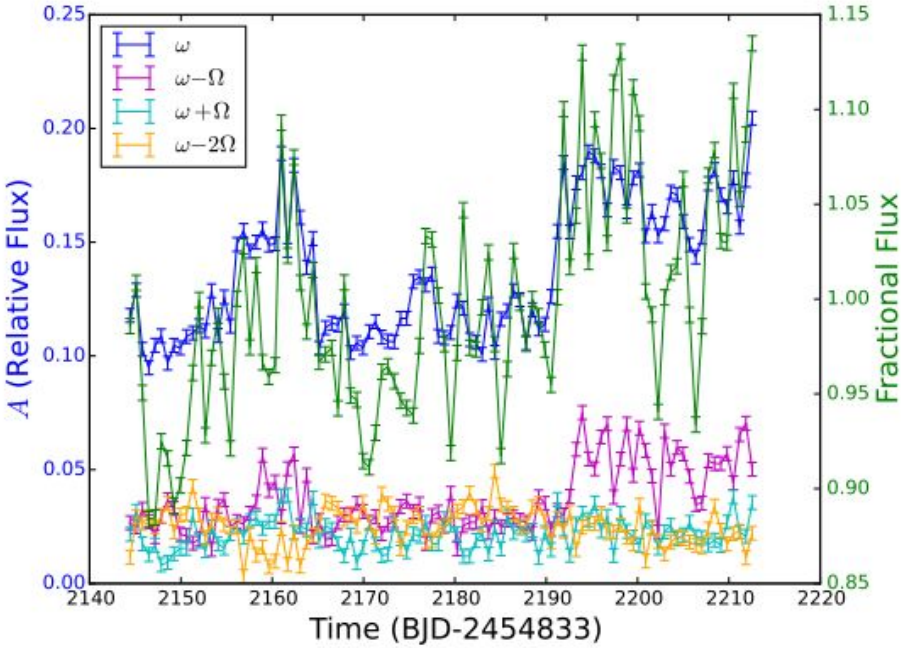

VATT observations in 2016

To further study the spin period in FO Aqr and study its changing accretion geometries, we took data using the VATT in April 2016 for a summer project.

We didn’t calibrate the data until June 2016…

Low State in FO Aqr

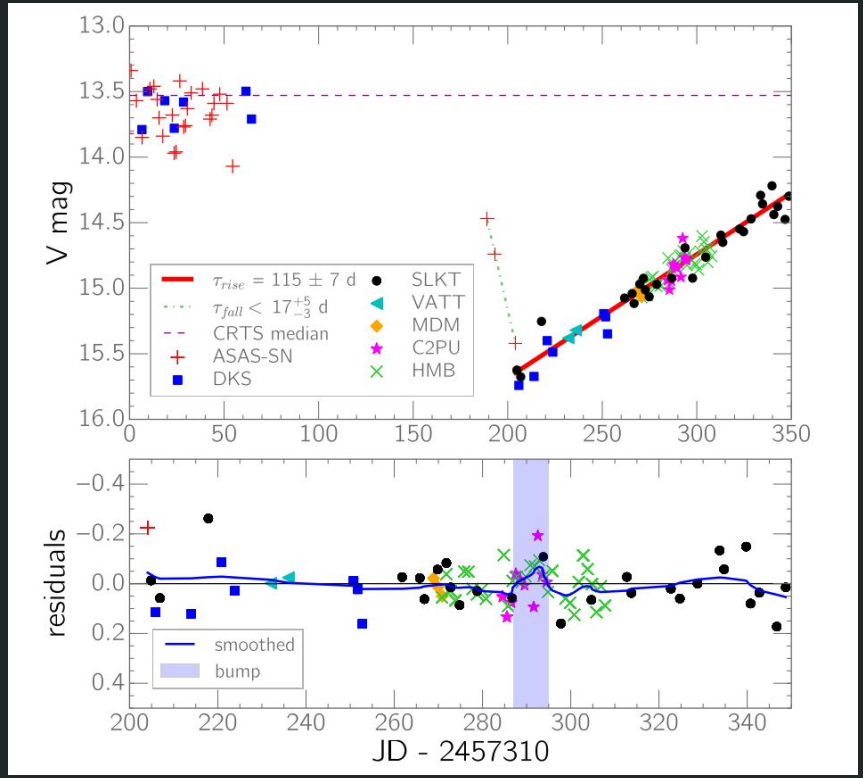

Low States in IPs

Thought to be due to a drop in the mass transfer rate due to star spots transiting the L1 point on the secondary.

FO Aquarii has never experienced one, with observations going back to 1927.

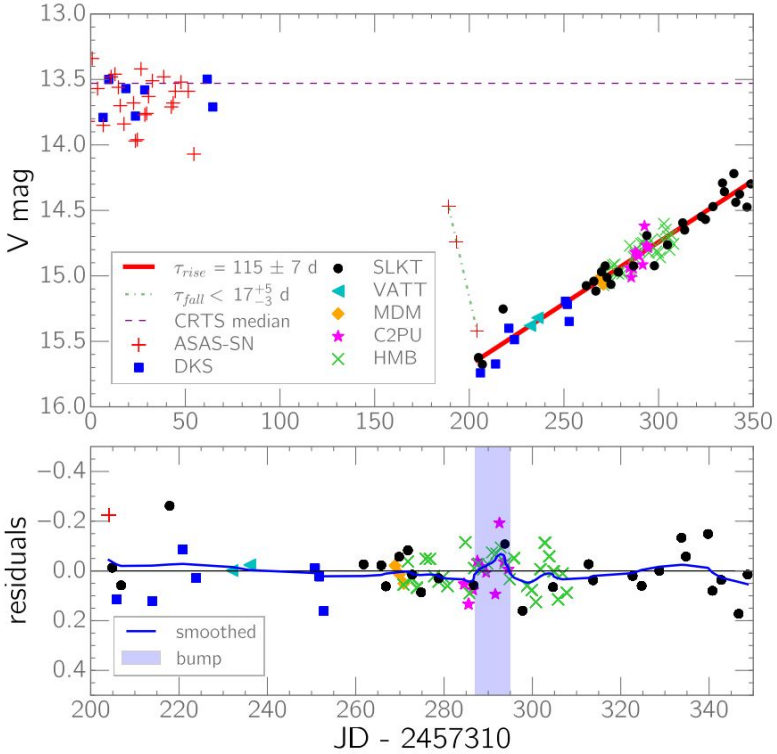

Observations of the low state

In June 2016, we realised FO Aqr was experiencing its first ever low state of accretion.

Observations taken by:

- Sarah L. Krizmanich Telescope (80 cm)
- VATT (1.8 m)
- McGrawhill Telescope at MDM (1.3 m)
- C2PU facility in Nice, France (1 m)
- Many members of the (AAVSO)
- Swift X-ray Observatory (July 2016)
- Chandra Observatory (July 2016)
- XMM-Newton (November 2016)

Optical Results

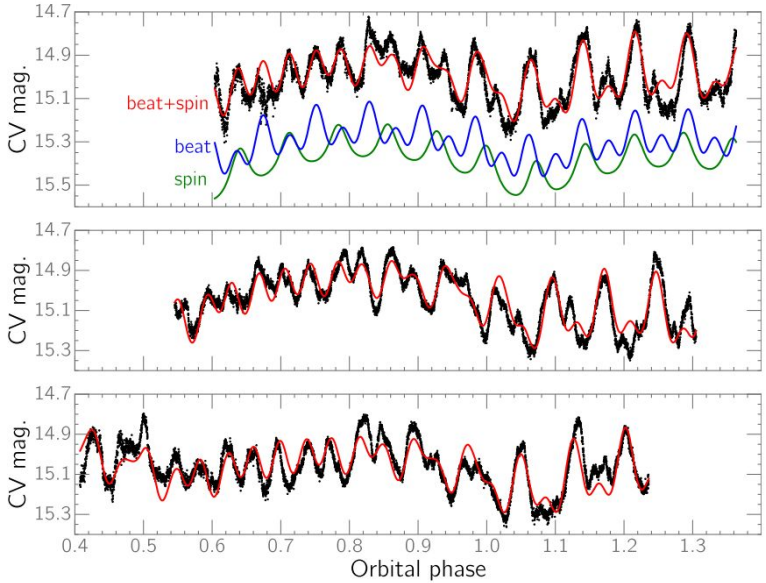

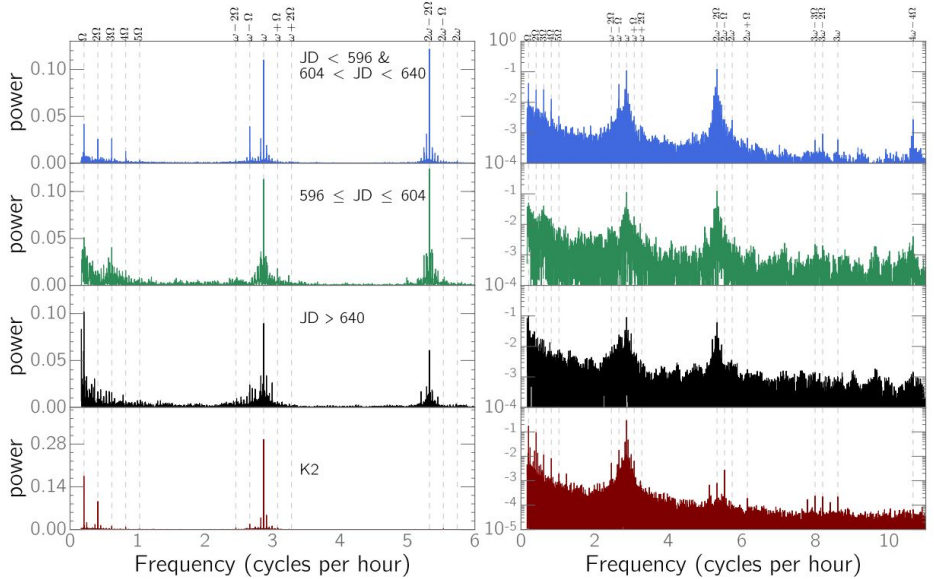

Swift 06 vs 16

Observations of FO Aqr taken in 2006 & 2016

2006 spectrum - weak soft component + strong hard component

2016 spectrum - strong soft component + weak hard component

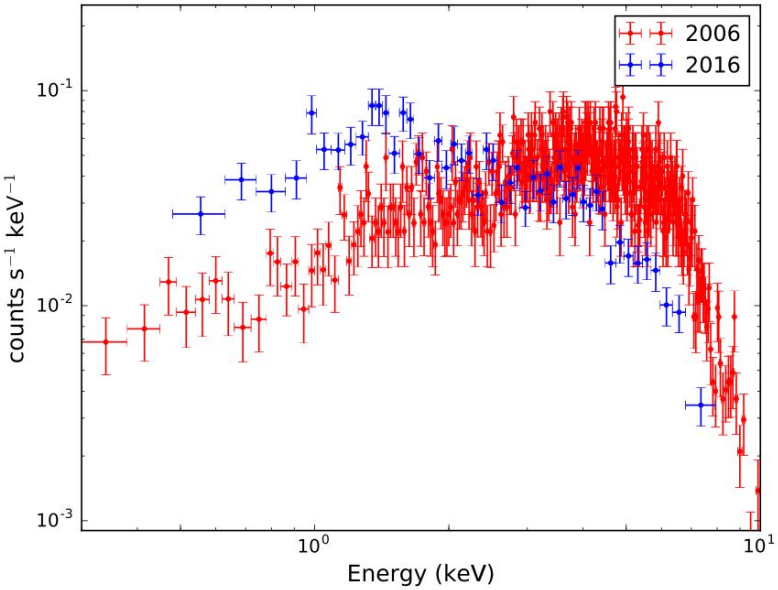

XMM 2001

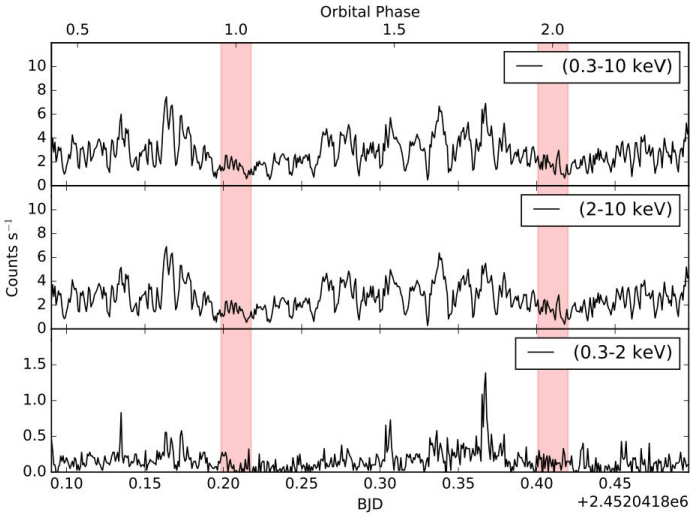

Chandra 2016

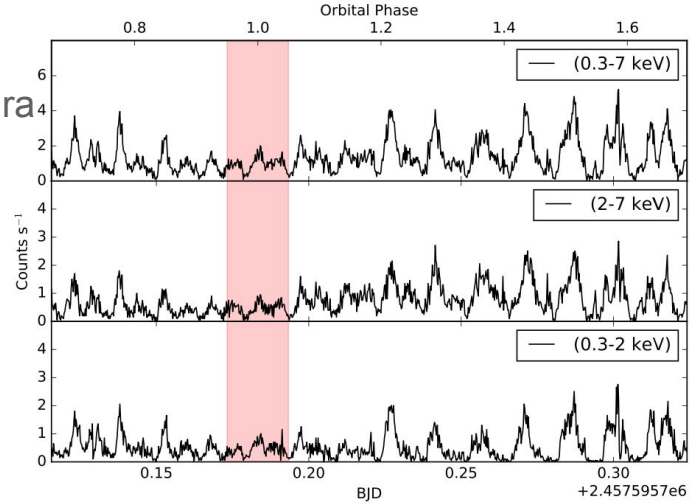

XMM 2016

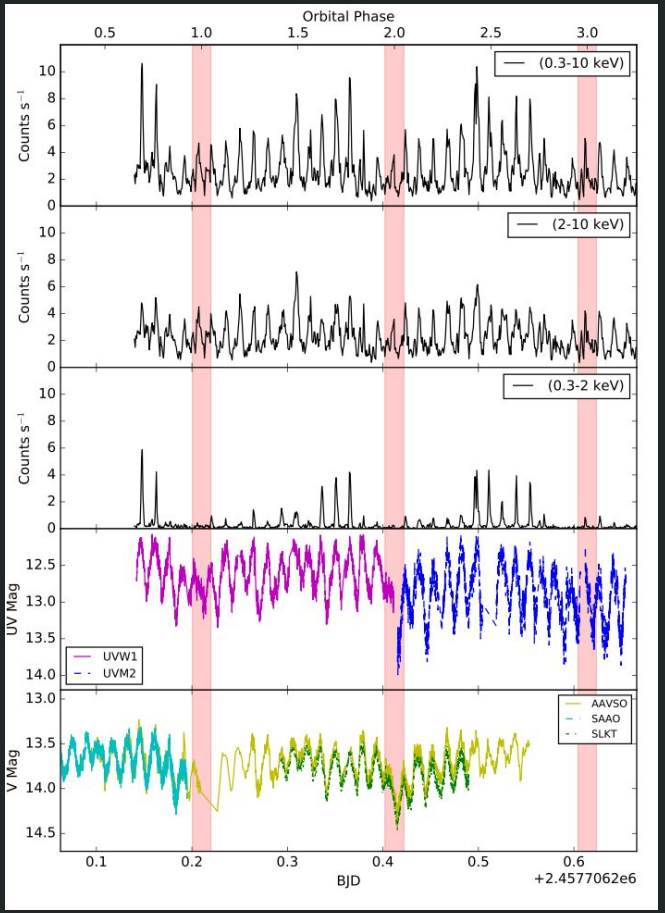

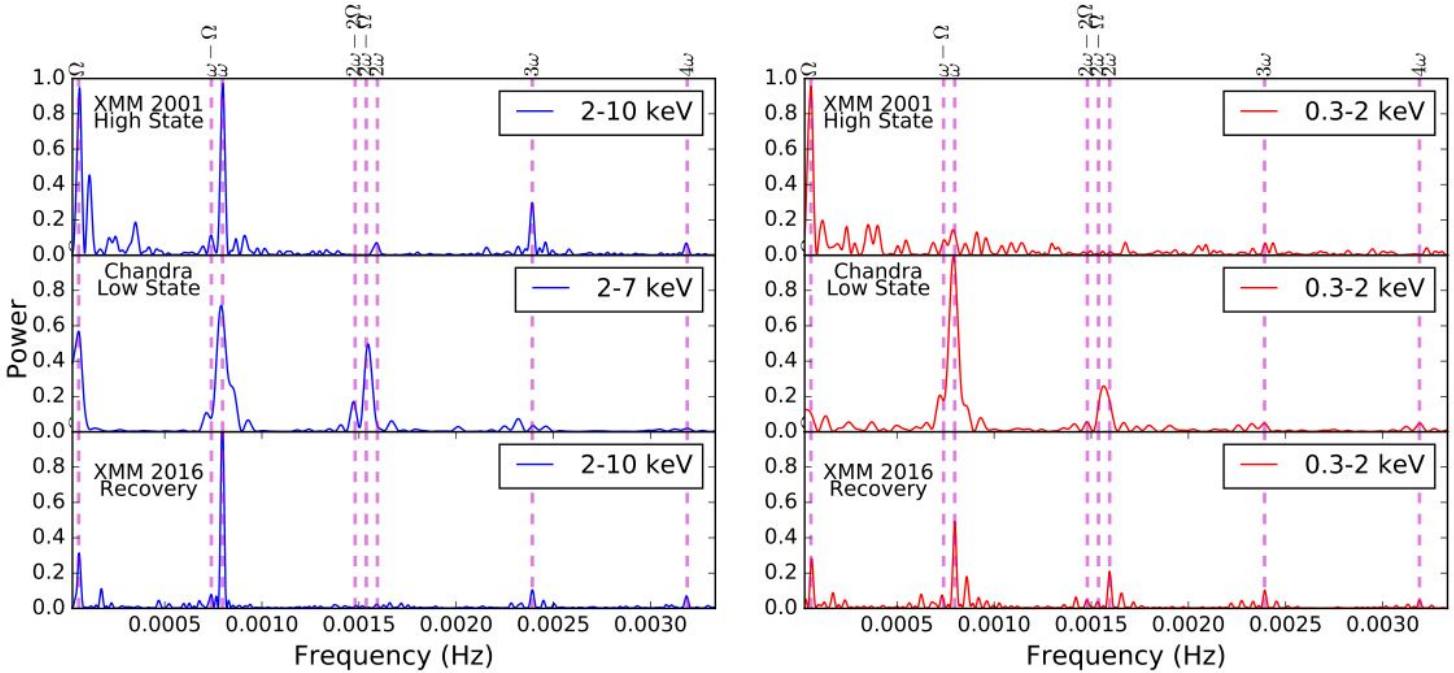

Power spectrum of X-ray data reveals the same changes in power as was seen in the optical data

Theoretical power spectra for discless accretors

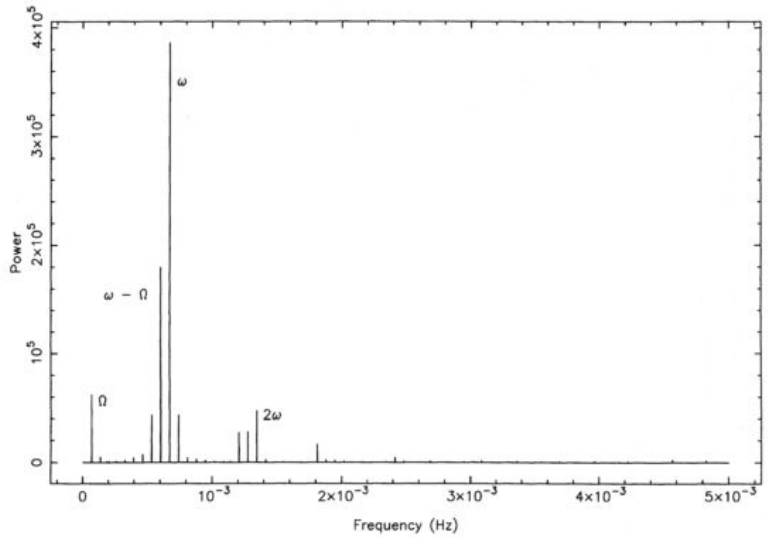

Inclination of 60 degrees, dipole offset of 20 degrees

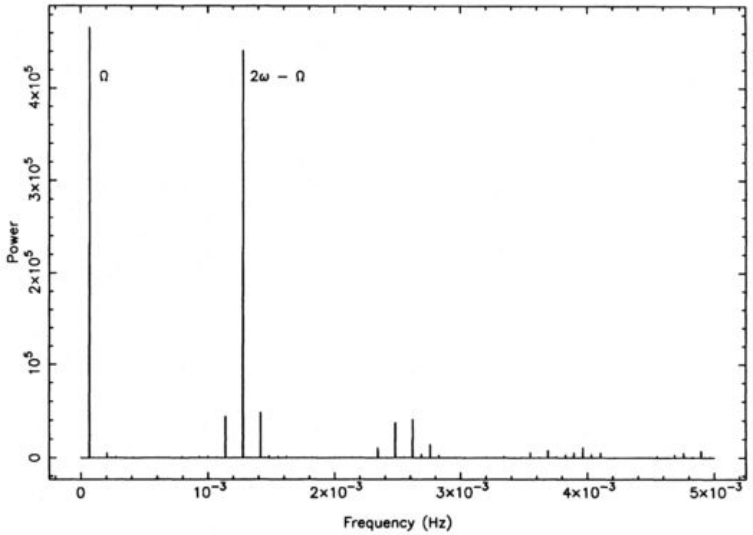

Inclination of 80 degrees, dipole offset of 80 degrees

From Wynn & King 1992, MNRAS, 255, 83

Changes to the X-ray Spectra

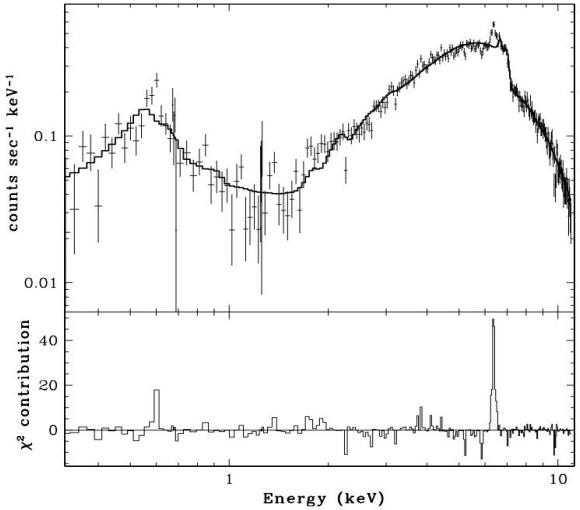

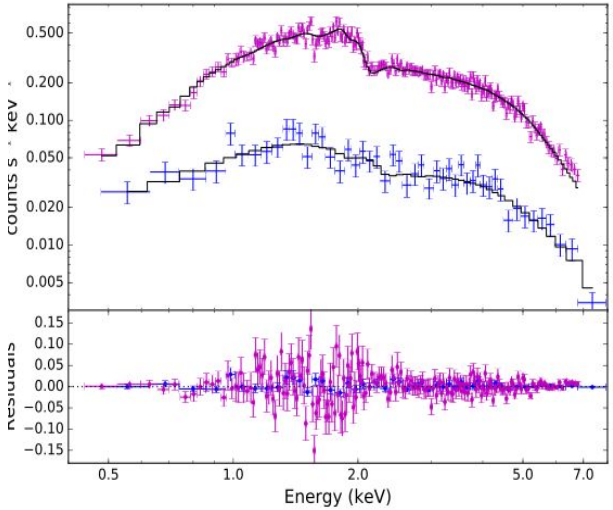

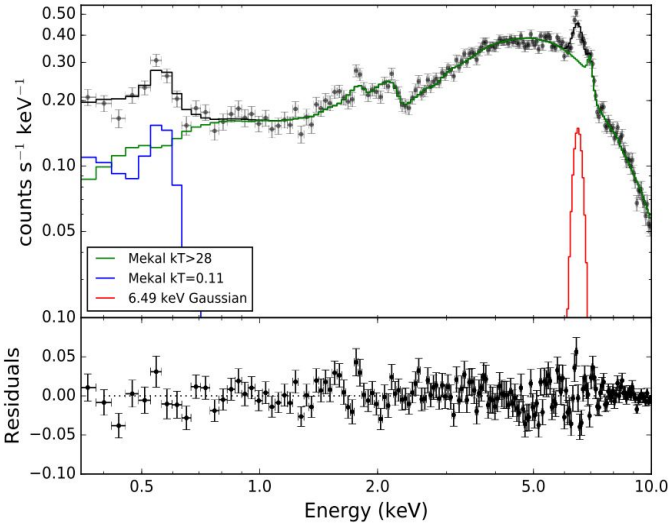

Length of the Recovery

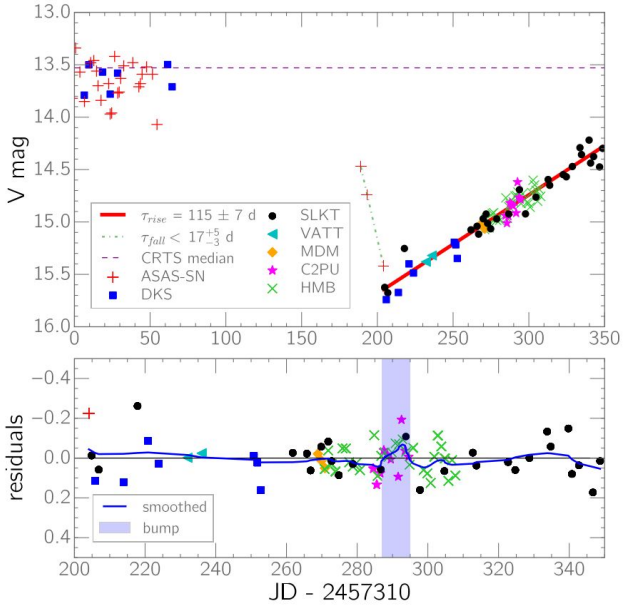

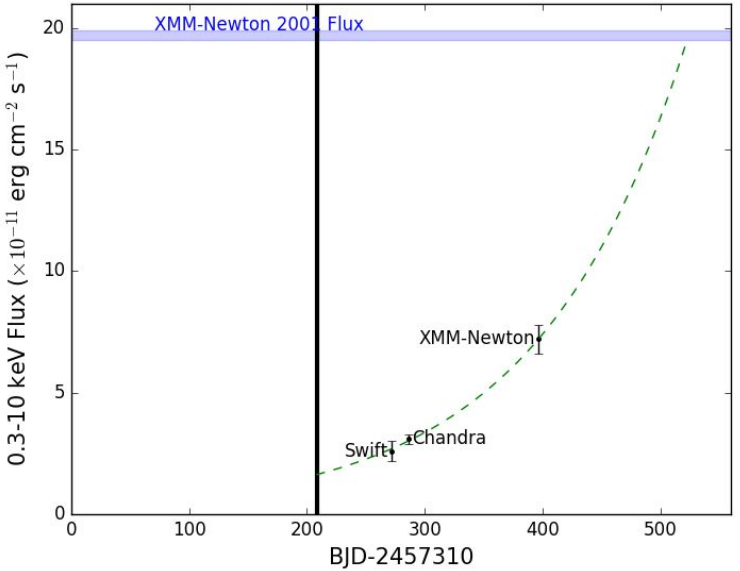

Low & Recovery Models

Component	Parameter	*Chandra* 2016	*Swift* 2016	*Swift* 2006	XMM 2016
TBABS (INTERSTELLAR)	N_H (10^{22} cm^{-2})	$0.02^{+0.08}_{-0.02}$	$0.05^{+0.2}_{-0.05}$	$0.78^{+0.19}_{0.18}$	$0.09^{+0.06}_{-0.04}$
TBABS (CIRCUMSTELLAR 1)	N_H (10^{22} cm^{-2})	$1.3^{+0.6}_{-0.3}$	$1.5^{+2.7}_{-0.7}$	$7.2^{+1.2}_{0.9}$	$15^{+3.0}_{-2.0}$
PARTCOV 1	cvf	$0.70^{+0.05}_{-0.08}$	$0.70^{+0.15}_{-0.26}$	$0.82^{+0.04}_{-0.03}$	$0.71^{+0.04}_{-0.05}$
TBABS (CIRCUMSTELLAR 2)	N_H (10^{22} cm^{-2})	-	-	-	$3.6^{+0.6}_{-0.5}$
PARTCOV 2	cvf	-	-	-	0.89±0.02
MEKAL	kT (keV)	>15	>7	-	>28
	Abundance	1.0	1.0	-	$0.5^{+0.3}_{-0.2}$
	norm	$0.160^{+0.365}_{-0.094}$	$0.83^{+1.5}_{-?}$	-	$0.037^{+0.002}_{-0.002}$
MEKAL	kT (keV)	-	-	-	$0.11^{+0.03}_{-0.02}$
	Abundance	-	-	-	$0.5^{+0.3}_{-0.2}$
	norm	-	-	-	$0.025^{+0.05}_{-0.02}$
BBODY	kT (keV)	-	-	61^{+8}_{-6}	-
BREMSS	kt (keV)	-	-	[29.7]	-
GAUSSIAN	Centre	-	-	-	$6.49^{+0.04}_{-0.02}$
	Sigma	-	-	-	$0.17^{+0.04}_{-0.05}$
	norm ($\times 10^{-4}$)	-	-	-	$1.3^{+0.3}_{-0.3}$
	χ^2_R	1.14	1.01	0.92	1.36

High Models

Component	Parameter (units)	Value	Error
Absorption	$n_{\rm H}$ (cm^{-2})	1.02×10^{21}	$^{+0.81\times10^{21}}_{-0.05\times10^{21}}$
Partial absn.	$n_{\rm H}$ (cm^{-2})	1.90×10^{23}	$^{+0.12\times10^{23}}_{-0.09\times10^{23}}$
	Cvr. fract	0.855	$^{+0.021}_{-0.026\times10^{-2}}$
Partial absn.	$n_{\rm H}$ (cm^{-2})	5.71×10^{22}	$^{+0.45\times10^{22}}_{-0.41\times10^{22}}$
	Cvr. fract	0.980	$^{+0.004}_{-0.005}$
Gaussian	Energy (keV)	6.40	Frozen
	Normalization	9.23×10^{-5}	$^{+0.695\times10^{-5}}_{-1.41\times10^{-5}}$
	Equiv. width (eV)	129	
Gaussian	Energy (keV)	0.587	$^{+0.031}_{-0.029}$
	Normalization	6.84×10^{-3}	$^{+4.69\times10^{-3}}_{-4.54\times10^{-3}}$
	Equiv. width (eV)	22.9	
Mekal	kT (keV)	0.176	$^{+0.024}_{-0.026}$
	Abundance	0.121	$^{+0.028}_{-0.023}$
	Normalization	0.160	$^{+0.365}_{-0.094}$
Mekal	kT (keV)	3.00	$^{+1.48}_{-0.73}$
	Normalization	3.32×10^{-2}	$^{+1.87\times10^{-2}}_{-1.51\times10^{-2}}$
Mekal	kT (keV)	13.9	$^{+6.5}_{-3.1}$
	Normalization	4.02×10^{-2}	$^{+0.88\times10^{-2}}_{-1.06\times10^{-2}}$

Soft X-ray pulses

Component	Parameter	Soft pulses	No Soft pulses
TBABS (INTERSTELLAR)	N_H (10^{22} cm^{-2})	0.10 ± 0.07	$0.07^{+0.09}_{-0.06}$
TBABS (CIRCUMSTELLAR 1)	N_H (10^{22} cm^{-2})	$13^{+6.0}_{-4.0}$	$15^{+3.0}_{-2.0}$
PARTCOV 1	cvf	$0.65^{+0.09}_{-0.11}$	0.74 ± 0.05
TBABS (CIRCUMSTELLAR 2)	N_H (10^{22} cm^{-2})	2.9 ± 1.0	$3.9^{+0.7}_{-0.6}$
PARTCOV 2	cvf	$0.81^{+0.04}_{-0.07}$	0.95 ± 0.01
MEKAL	kT (keV)	>20	> 29
	Abundance	$0.3^{+0.5}_{-0.25}$	$0.5^{+0.4}_{-0.3}$
	norm	$0.036^{+0.005}_{-0.003}$	0.037 ± 0.002
MEKAL	kT (keV)	<0.13	$0.12^{+0.05}_{-0.03}$
	Abundance	$0.3^{+0.5}_{-0.25}$	$0.5^{+0.4}_{-0.3}$
	norm	$0.05^{+0.2}_{-0.04}$	$0.02^{+0.05}_{-0.01}$
GAUSSIAN	Centre	$6.49^{+0.07}_{-0.05}$	$6.05^{+0.05}_{-0.04}$
	Sigma	$0.17^{+0.10}_{-0.07}$	$0.18^{+0.08}_{-0.05}$
	norm ($\times10^{-4}$)	$1.3^{+0.5}_{-0.4}$	1.3 ± 0.3
	χ^2_R	1.23	1.38

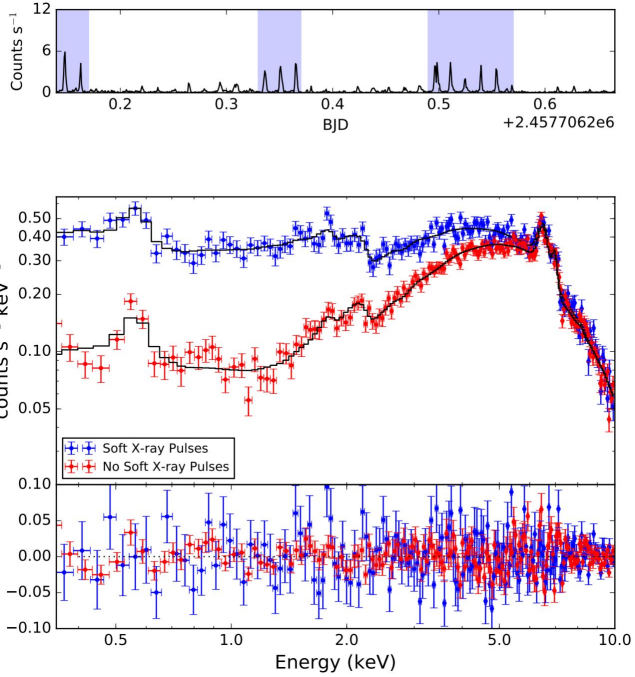

Differences between recovery and high state

Same structure for both pulses with an added phase shift.

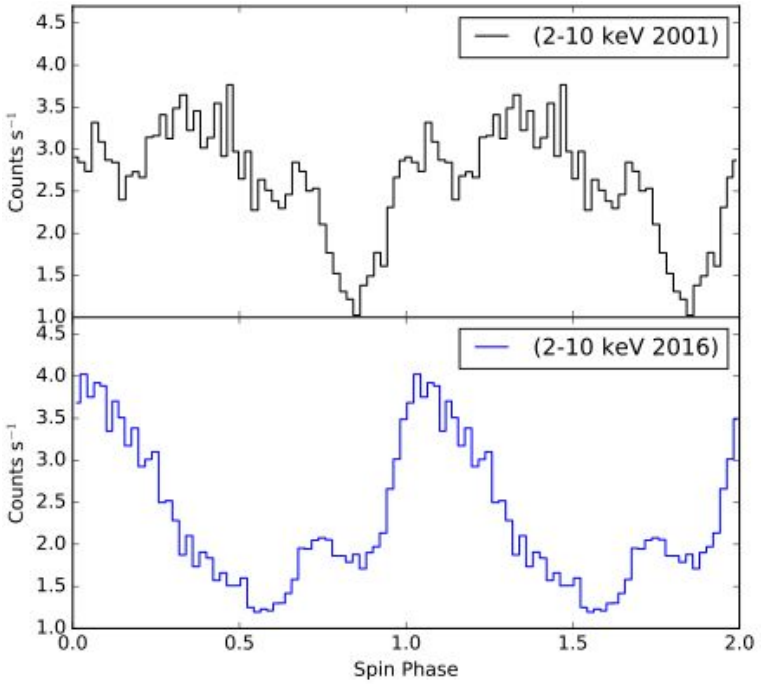

Conclusions

FO Aquarii has an incredibly complex spin history, but is likely spinning close to its equilibrium value.

The first X-ray observations of an IP in a low state have shown that the accretion geometry undergoes significant changes during the low state.

Further X-ray observations were taken on May 12th, after FO Aquarii had come out from behind the Sun. These observations are currently being analysed to confirm FO Aq has returned to business as usual.

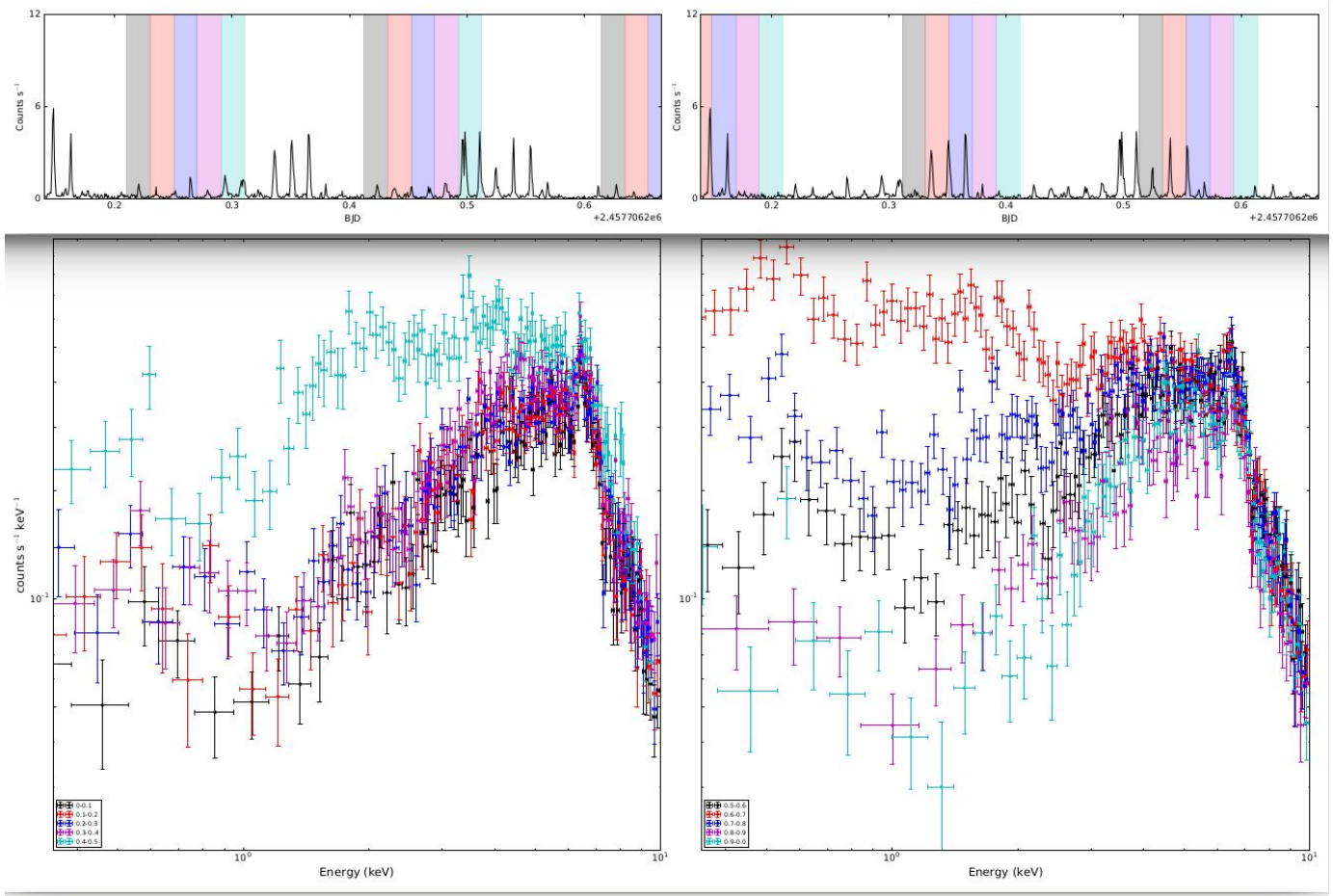
Counts s⁻¹
BJD
+2.4577062e6
counts s⁻² keV⁻¹
Energy (keV)

Accretion geometries & power spectra

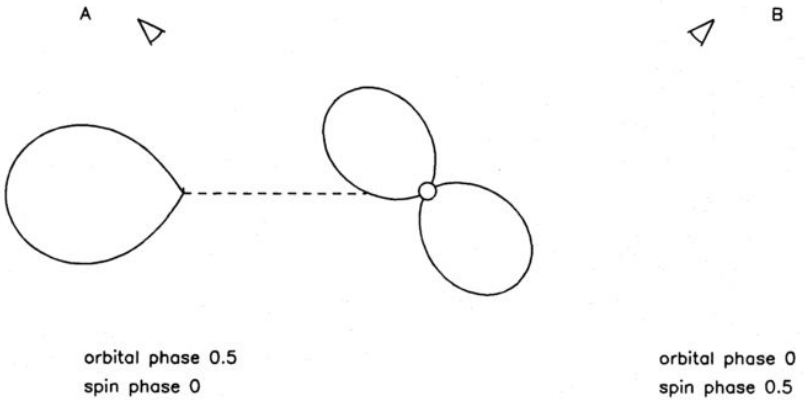

Wynn & King, 1992 MNRAS, 255 ,83

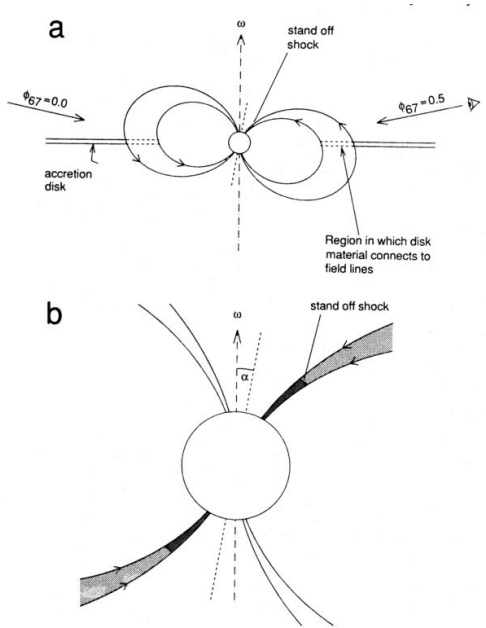

Rosen, Mason, & Cordóva, 1988, MNRAS, 231, 549